

Phase separation and competition of superconductivity and magnetism in the two-dimensional Hubbard model: From strong to weak coupling

M. Aichhorn,^{1,*} E. Arrighi,² M. Potthoff,³ and W. Hanke^{1,4}

¹*Institute for Theoretical Physics and Astrophysics, University of Würzburg, Am Hubland, 97074 Würzburg, Germany*

²*Institute of Theoretical Physics and Computational Physics, TU Graz, Petersgasse 16, 8010 Graz, Austria*

³*I. Institute for Theoretical Physics, University of Hamburg, Jungiusstraße 9, 20355 Hamburg, Germany*

⁴*Kavli Institute for Theoretical Physics, University of California, Santa Barbara, California 93106, USA*

(Received 24 July 2007; revised manuscript received 18 October 2007; published 11 December 2007)

Cooperation and competition between the antiferromagnetic, d -wave superconducting, and Mott-insulating states are explored for the two-dimensional Hubbard model including nearest and next-nearest-neighbor hoppings at zero temperature. Using the variational cluster approach with clusters of different shapes and sizes up to 10 sites, it is found that the doping-driven transition from a phase with microscopic coexistence of antiferromagnetism and superconductivity to a purely superconducting phase is discontinuous for strong interaction and accompanied by phase separation. At half-filling the system is in an antiferromagnetic Mott-insulating state with vanishing charge compressibility. Upon decreasing the interaction strength U below a certain critical value of roughly $U_c \sim 4$ (in units of the nearest-neighbor hopping), however, the filling-dependent magnetic transition changes its character and becomes continuous. Phase separation or, more carefully, the tendency towards the formation of inhomogeneous states disappears. This critical value is in contrast to previous studies, where a much larger value was obtained. Moreover, we find that the system at half-filling undergoes the Mott transition from an insulator to a state with a finite charge compressibility *at essentially the same value*. The weakly correlated state at half-filling exhibits superconductivity microscopically admixed to the antiferromagnetic order. This scenario suggests a close relation between phase separation and the Mott-insulator physics.

DOI: [10.1103/PhysRevB.76.224509](https://doi.org/10.1103/PhysRevB.76.224509)

PACS number(s): 74.20.-z, 71.10.Hf

I. INTRODUCTION

One of the standard models in theoretical studies of high-temperature superconductors is the single-band Hubbard model. Substantial progress in the understanding of its ground-state properties in two dimensions has been achieved by applying dynamical quantum-cluster approaches,¹ such as the dynamical cluster approximation,² the cellular dynamical mean-field theory^{3,4} or the variational cluster approach (VCA).⁵ Several studies predict d -wave superconductivity at low⁶ or zero temperatures^{7–11} for intermediate interaction strengths of the order of the free bandwidth.

Experimentally, it is well known that cuprate-based high- T_C compounds at low doping concentrations tend to form charge and spin inhomogeneities, such as stripe^{12,13} or checkerboard modulations.^{14–17} An unbiased theoretical study of inhomogeneous phases is hardly possible within quantum-cluster approaches for the presently accessible cluster sizes. Furthermore, for a realistic modeling of charge inhomogeneities additional nonlocal interaction terms should actually be taken into account.^{18–20} However, by searching for phase separation, an overall tendency towards the formation of inhomogeneous phases can easily and reliably be detected even if only homogeneous solutions are allowed within the cluster mean-field calculation.

Phase separation (PS), i.e., separation into two homogeneous *macroscopic* regions with different thermodynamical properties, is the most simple kind of inhomogeneity. It has been argued^{18,20} that phase separation occurring in Hubbard- or t - J -type models with short-range interactions only, can transform to *microscopically* inhomogeneous structures, such as stripes, when long-range repulsions were included.¹⁹ For

this reason, the investigation of PS in the Hubbard model is a reasonable starting point for an understanding of inhomogeneous phases in the high- T_C cuprate materials.

The occurrence of phase separation in the Hubbard model has been investigated in the past using several different techniques. Calculations for finite clusters using quantum Monte Carlo techniques^{21,22} found no evidence for PS in the Hubbard model with nearest-neighbor hopping only. Different results have been obtained in infinite dimensions within dynamical mean-field theory (DMFT) where PS has been reported.^{23–25} PS has also been discussed in the context of *marginal quantum criticality*,^{26,27} where PS occurs at the first-order side of the marginal quantum critical point (MQCP). For the two-dimensional model including hopping between next-nearest neighbors, calculations within the dynamical cluster approximation yield phase separation in the paramagnetic state.²⁸ VCA and cellular DMFT studies predict phase separation between a phase with long-range antiferromagnetic (AF) order at low doping and a superconducting (SC) state at high doping.^{8–11}

The new aspect of our work is to systematically investigate the fate of the phase-separated state within VCA when decreasing the interaction strength. We demonstrate by using as reference systems a variety of cluster sizes up to 10 sites, that the tendency towards PS is lost at small U of the order of $U_c \sim 4$. Above of this value we found strong evidence from this systematic study that the inhomogeneous state is indeed present in the thermodynamic limit.

In previous cellular DMFT work,¹¹ a transition which is in certain aspects similar to ours was found around $U_c \approx 8$, using 2×2 clusters only. According to previous studies^{29–31} it is known, however, that a physical transition for the 2D Hub-

bard model is taking place at much smaller values, $U \approx 4$. Here, the two separate energy scales U and J are eventually merging, as exemplified by the transition from two energy bands (coherent low-lying and incoherent Hubbard bands) to just one single band. A motivation for our study was partly to investigate the relation between the metal-to-insulator transition and PS. Most strikingly, we find that the transition to a metallic state at half-filling occurs *at essentially the same value of U* , below which PS disappears. This strongly suggests a definite relation between PS and the Mott insulator, a relation that was previously speculated about.³²

The paper is organized as follows. In Sec. II, we introduce the model and briefly review the variational cluster approximation. In Sec. III, our results are presented and discussed. The conclusions are summarized in Sec. IV.

II. THEORY

Using standard notations, the Hubbard model is given by $H = H_0(t) + H_1$ where

$$H_0(t) = -t_{\text{NN}} \sum_{\langle ij \rangle, \sigma} c_{i\sigma}^\dagger c_{j\sigma} - t_{\text{NNN}} \sum_{\langle\langle ij \rangle\rangle, \sigma} c_{i\sigma}^\dagger c_{j\sigma}, \quad (1)$$

$$H_1 = U \sum_i n_{i\uparrow} n_{i\downarrow}. \quad (2)$$

The operator $c_{i\sigma}^{(\dagger)}$ creates (annihilates) an electron with spin σ at the site i , and $n_{i\sigma}$ is the corresponding occupation number operator. We consider both hopping t_{NN} along nearest-neighbor bonds $\langle ij \rangle$ as well as hopping t_{NNN} along next-nearest-neighbor bonds $\langle\langle ij \rangle\rangle$. U is the local Coulomb interaction. We set the unit of energy by t_{NN} and choose $t_{\text{NNN}} = -0.3t_{\text{NN}}$ throughout the paper which is a realistic value for the cuprate materials.

The main idea of the variational-cluster approximation^{5,33} (VCA) is to consider a “reference system” to span a space of trial self-energies among which the self-energy that describes best the physics of the infinite-size lattice model is obtained via a dynamical variational principle $\delta\Omega[\Sigma] = 0$. Here Ω stands for the grand potential. The reference system is given by a Hamiltonian H' with the same interaction part H_1 as the physical system but with modified one-particle parameters t' , i.e., $H' = H_0(t') + H_1$. Within the VCA one takes as a reference system a lattice split up into isolated clusters of a given size. Thereby, the effects of short-range correlations on the self-energy are included on a scale given by the cluster extension. Trial self-energies $\Sigma = \Sigma(t')$ are varied by varying the parameters t' . Inserting the trial self-energy into the self-energy functional generates a function $\Omega(t') = \Omega[\Sigma(t')]$ the stationary points of which we are interested in. It can be shown^{5,33} that

$$\Omega(t') = \Omega' + \text{Tr} \ln[G_{0,t}^{-1} - \Sigma(t')]^{-1} - \text{Tr} \ln G_{t'}, \quad (3)$$

where Ω' is the grand potential and $G_{t'}$ the Green's function of the reference system and $G_{0,t}$ the noninteracting Green's function of the physical system. While $G_{0,t}$ is easily accessible, we calculate the reference system's properties using full diagonalization for small clusters, and the band Lanczos

methods for larger ones. A description of the numerical details can be found in Ref. 10.

Since we are interested in PS involving symmetry-broken antiferromagnetic and d -wave superconducting phases, our reference system includes the corresponding (fictitious) symmetry-breaking fields,

$$H'_{\text{AF}} = h'_{\text{AF}} \sum_{i\sigma} (n_{i\uparrow} - n_{i\downarrow}) e^{i\mathbf{Q}\mathbf{R}_i}, \quad (4a)$$

$$H'_{\text{SC}} = h'_{\text{SC}} \sum_{ij} \frac{\eta_{ij}}{2} (c_{i\uparrow} c_{j\downarrow} + \text{H.c.}), \quad (4b)$$

where h'_{AF} and h'_{SC} are the strengths of a staggered magnetic and of a nearest-neighbor d -wave pairing “Weiss” field, respectively. Furthermore, $\mathbf{Q} = (\pi, \pi)$ is the AF wave vector, and η_{ij} denotes the d -wave form factor which is equal to +1 (−1) for nearest-neighbor sites with $\mathbf{R}_i - \mathbf{R}_j$ in x (y) direction. In addition, an on-site potential is included in the set of variational parameters to ensure a thermodynamically consistent determination of the average particle number.⁹ Note that all three variational parameters couple to one-particle operators only.

III. RESULTS

For the calculations we concentrate on the hole-doped side of the phase diagram since it has been shown that there PS is much more pronounced than in the electron-doped case.^{8–10} The occurrence of PS can be best inferred from the dependence of the chemical potential on the particle number. For a physical system in thermodynamical equilibrium the charge susceptibility $\kappa = \partial n / \partial \mu$ must be non-negative. Hence, $\kappa < 0$ indicates a thermodynamically unstable phase. At a fixed *average* density n lying in the instability region $n_1 < n < n_2$, the free energy can be reduced if the system develops two spatially separated homogeneous phases, one with a fraction $x = (n_2 - n) / (n_2 - n_1)$ of particles at the density $n_1 < n$ and another one with the fraction $1 - x$ at $n_2 > n$, rather than having a single homogeneous phase. The boundaries n_1 and n_2 of the instability region can be obtained by a Maxwell construction (see Fig. 1), in close analogy to a gas-liquid system. After the Maxwell construction, the *physical* chemical potential is independent of n between n_1 and n_2 .

In Fig. 1 we show results for the interrelation of the chemical potential μ and the average density n as a function of Coulomb interaction U . The calculations have been done with a 2×2 cluster as a reference system. In the strong coupling regime, $U = 12$, we find that the chemical potential μ as function of the density n shows a nonmonotonic behavior (and thus $\kappa < 0$) as mentioned above. We conclude that for this coupling and within the precision set by the 2×2 cluster reference system, the results imply PS into an AF+SC mixed phase^{34,40,41} at low doping and a purely SC phase at higher doping. The critical chemical potential where the two phases coexist, is indicated by a horizontal dotted line in Fig. 1. This behavior is very similar to the previously reported one for $U = 8$.^{9,10} For comparison, results for $U = 8$ —as published in Ref. 9—are shown in Fig. 1 in the middle panel.

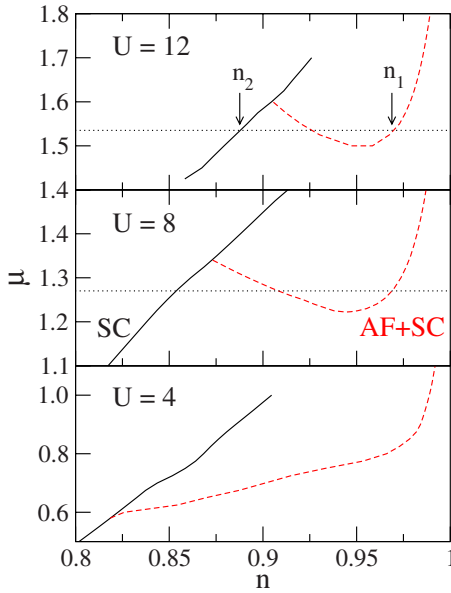


FIG. 1. (Color online) Chemical potential μ as function of the average density n , calculated with a 2×2 cluster as reference system for different values of U . From top to bottom: $U=12$, 8, and 4, respectively. n_1 and n_2 denote the boundaries of the instability (PS) region. Solid lines: Pure SC phase. Dashed lines: AF+SC mixed phase. Dotted horizontal line: Critical chemical potential (where applicable).

The picture changes even qualitatively when going to weak interactions, e.g., $U=4$. As shown in the lower panel of Fig. 1, the chemical potential as function of n shows a positive slope for all dopings, without an intermediate region with negative sign. We conclude that for weak interaction there is no tendency to the formation of inhomogeneities, even for the smallest cluster we used for our calculations. Instead, the AF+SC solution is stable up to larger dopings, and the staggered magnetization vanishes continuously in the stable and homogeneous solution.

Since the occurrence of PS is subject to rather strong finite-size effects,¹⁰ and in order to further elucidate the difference between the coupling regimes, we have recalculated the phase diagram using larger clusters with $L_c=8$ and $L_c=10$ lattice sites as reference systems (see Fig. 2). For both $L_c=8$ and 10 we have considered two different cluster geometries to estimate dependencies on the cluster shape.

In addition to the boundaries of the instability region, n_1 and n_2 , we define a characteristic energy $\Delta\mu = \mu^* - \mu_c$. Here, μ^* is defined as the point where the slope of $\mu(n)$ changes sign, and μ_c is the critical chemical potential, i. e., the point at which $\Omega_{AF+SC}(\mu)$ crosses $\Omega_{SC}(\mu)$. Equivalently, μ_c is fixed by the Maxwell construction, see Fig. 1. In the limit of infinite cluster size, the characteristic energy $\Delta\mu$ must vanish as the reference system (and thereby also the original system) is solved exactly within the VCA: For $L_c \rightarrow \infty$ (and for densities in the exact instability region) the reference system spontaneously generates the phase-separated state, and $\mu(n)$ becomes flat between n_1 and n_2 , as discussed above. On the other hand, the difference between the critical densities $n_2 - n_1$ must converge to a nonzero value for $L_c \rightarrow \infty$ whenever

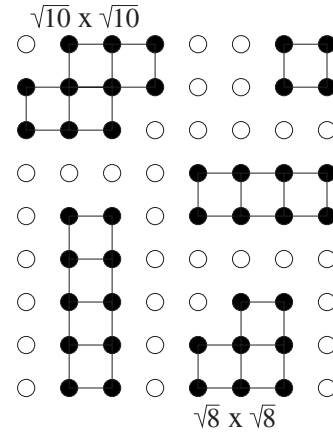


FIG. 2. Clusters used as reference systems in this study. The “ $\sqrt{10} \times \sqrt{10}$ ” and “ $\sqrt{8} \times \sqrt{8}$ ” clusters are marked explicitly in the figure.

the system in the thermodynamic limit shows phase separation. Notice that the difference between the grand potentials Ω_{AF+SC} and Ω_{SC} becomes smaller and smaller with increasing cluster size. Thus, together with the increasing numerical effort, this makes the identification of $\Delta\mu$ harder for larger clusters. Contrary, the slope of $\Omega(\mu)$, i.e., the particle density, is not affected by a systematic shift and, therefore, its calculation is quite reliable also for larger L_c .

Results for these quantities are shown in Fig. 3. The upper panel shows $\Delta\mu$ as a function of the Hubbard interaction U . As expected from the discussion above, $\Delta\mu$ decreases for increasing cluster size. Quite surprising, however, is the dependence of $\Delta\mu$ on the interaction.

As $\Delta\mu \neq 0$ is a finite-size effect, one could expect $\Delta\mu$ to be smaller for stronger interactions since a cluster mean-field

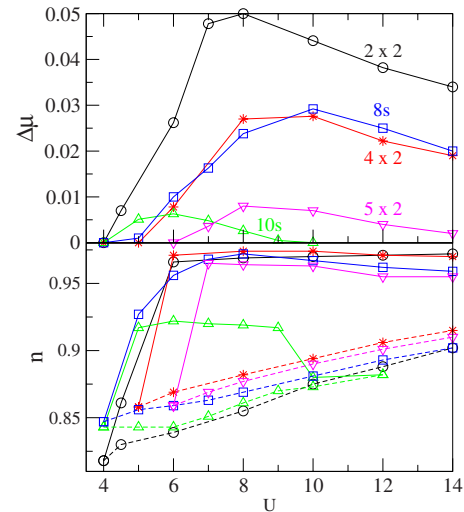


FIG. 3. (Color online) Characteristic energy $\Delta\mu = \mu^* - \mu_c$ (top) and critical densities n_1 and n_2 (bottom) as functions of U , calculated using the clusters shown in Fig. 2 as reference systems, 2×2 (circles), $\sqrt{8} \times \sqrt{8}$ (squares), 4×2 (stars), 5×2 (triangles down), and $\sqrt{10} \times \sqrt{10}$ (triangles up). Lower plot: Solid lines correspond to the critical density n_1 and dashed lines to the critical density n_2 .

approach quite generally is expected to be more reliable in the strong-coupling than in the weak-coupling regime. At least, it is known from previous calculations³⁵ that for weaker interactions finite-size effects are larger as could be seen from the stronger dependence of the optimal variational parameters on the size of the reference system cluster. In fact, we find for large U (see Fig. 3) that $\Delta\mu$ increases with decreasing interaction. Below $U \approx 10$, however, $\Delta\mu$ starts to decrease and eventually even vanishes at some critical value U_c (which exhibits a finite but weak dependence on the cluster size). This decrease indicates a qualitative change of the phase transition with decreasing U .

From the analysis of the critical densities we see that the vanishing of $\Delta\mu$ corresponds to the disappearance of the phase-separated state: The critical densities n_1 and n_2 of the two coexisting phases are shown in the lower panel of Fig. 3. The dependence of their difference $n_2 - n_1$ on U closely resembles the dependence of $\Delta\mu$. In particular, for U below some U_c , n_1 and n_2 collapse to a single point, i.e., phase separation disappears.

It is encouraging to see that, except for the $\sqrt{10} \times \sqrt{10}$ cluster, the critical densities shown in this plot depend only very weakly on the cluster size. The $\sqrt{10} \times \sqrt{10}$ cluster seems to behave differently. Probably, its shape (see Fig. 2) makes this cluster unsuitable for finite-size scaling. This is also confirmed by the fact that $\Delta\mu$ does not display the correct scaling behavior for this cluster. In addition, the 5×2 cluster with the same number of sites $L_c = 10$ does display the correct L_c dependence of $\Delta\mu$. Excluding the results from the $\sqrt{10} \times \sqrt{10}$ cluster, n_1 and n_2 show a very weak dependence on L_c . Close to U_c , the L_c dependence is somewhat stronger again which is not surprising, of course.

In view of the results for different interaction strengths and cluster sizes we conclude that PS persists in the thermodynamic limit down to a critical interaction U_c . Admittedly, there is a rather large uncertainty in the determination of U_c : Estimates range between $U_c \sim 4$ and $U_c \sim 6$. Interestingly, results from the $\sqrt{10} \times \sqrt{10}$ cluster do not only show a lower critical interaction but also an upper critical value $U_{c2} \approx 10$ above which PS disappears. As discussed above, however, the question is whether results for this cluster shape are reliable or not.

From the grand potential we can extract the ground-state energy of the system by $E_0 = \Omega + \mu N$. Results for the ground-state energy per site, i.e., E_0/L , are shown in Fig. 4 for $U=4, 8$, and 12 , respectively. Although some (small) finite-size effects are visible, the ground-state energy seems to be well converged in our approach. As a check for consistency we found that the general relation $\partial(E_0/L)/\partial n = \mu$ is fulfilled within numerical accuracy. This relation is a consequence of the Legendre transformation $E_0 = \Omega + \mu N$ and must be true in all calculations independent of the cluster used as a reference system.

The filling dependence of the order parameters is displayed in Fig. 5. Although some finite-size effects are visible, the results strongly indicate that superconductivity persists in the thermodynamic limit. We can also extract an interesting trend when comparing the results for $U=8$ with those for $U=4$: While the staggered magnetization *decreases* the SC order parameter *increases* with decreasing U . At the same

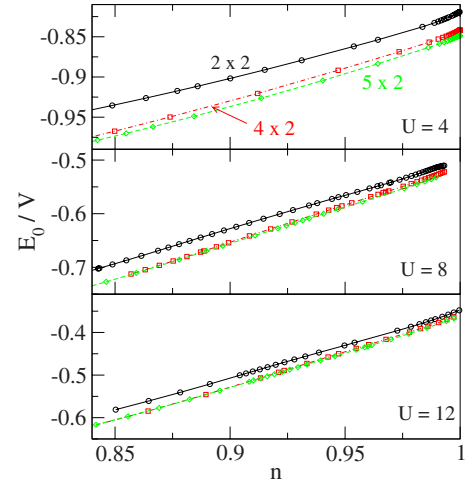


FIG. 4. (Color online) Ground-state energy per site E_0/L as function of electron density n , for $U=4$ (top), $U=8$ (middle), and $U=12$ (bottom). Results are shown for the 2×2 (solid), 4×2 (dashed-dotted), and 5×2 (dashed) reference systems.

time the doping region where a magnetic solution exists, extends to somewhat larger dopings for smaller U . Another difference is the small but finite value of the dSC order parameter at half-filling ($n=1$) for $U=4$, as can be seen in the lower right plot of Fig. 5. This is directly related to the closing of the Mott-Hubbard gap, as discussed below.

There are also some differences between $U=8$ and $U=12$, although they are considerably smaller. Taking for instance the boundary of the AF phase, i.e., the density where the AF order parameter vanishes, it is at $n \approx 0.82$ for $U=4$, $n \approx 0.87$ for $U=8$, and $n \approx 0.89$ for $U=12$. Also the changes of the SC order parameter are very small. We want to stress again that the major difference, however, is the *absence* of PS for $U=4$; see Figs. 1 and 4.

To understand the occurrence of a critical interaction for PS as well as the finite dSC order parameter at half-filling,

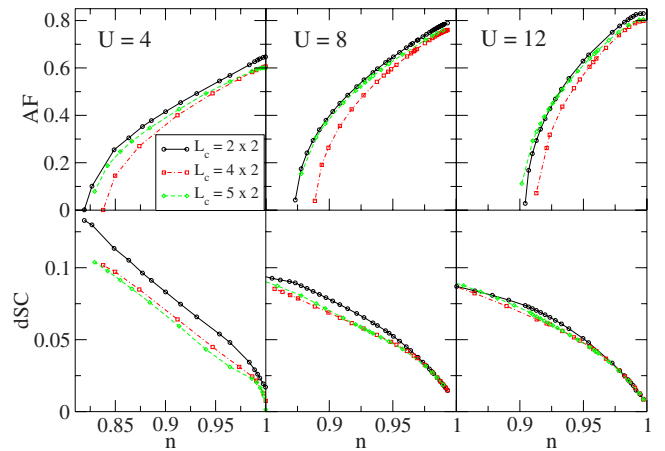


FIG. 5. (Color online) Order parameters as a function of density for $U=4$ (left), $U=8$ (middle), and $U=12$ (right). Top: AF order parameter. Bottom: d -wave SC order parameter. Results are shown for the 2×2 (solid), 4×2 (dashed-dotted), and 5×2 (dashed) reference systems.

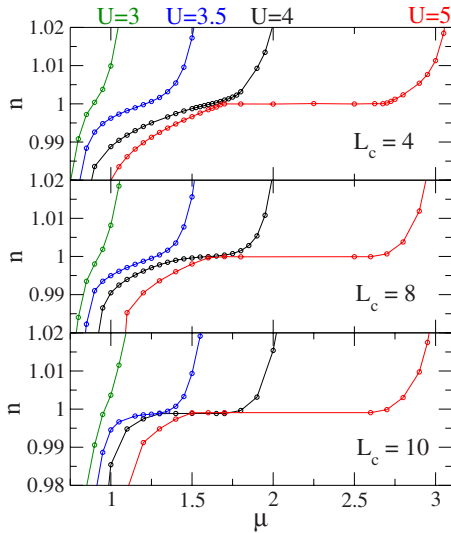


FIG. 6. (Color online) Closing of the Mott gap as function of U . From top to bottom: $L_c=2 \times 2$, $L_c=4 \times 2$, and $L_c=\sqrt{10} \times \sqrt{10}$ site clusters. From left to right: $U=3$ (green), 3.5 (blue), 4 (black), and 5 (red).

we study the $n(\mu)$ behavior close to half-filling as a function of U . Results are shown in Fig. 6 in the vicinity of $n=1$. For $U=5$ there is a flat $n(\mu)$ dependence for a finite range of chemical potentials, i.e., a vanishing charge susceptibility $\kappa=0$. This indicates the presence of an (AF) Mott insulating state at half-filling. The Mott gap shrinks with decreasing U , and eventually the system shows metallic behavior at $n=1$. This agrees well with previous results.^{30,31,36,37} For the smallest system the transition to the metal takes place at an interaction strength somewhat above $U=4$, whereas for larger clusters the critical U is shifted to slightly smaller values. For the 5×2 cluster (not shown) it is slightly below $U=4$, and for the $\sqrt{10} \times \sqrt{10}$ cluster the transition takes place slightly above $U=3.5$. Notice that the value of U where the gap closes can also be read off directly from the dSC order parameter. Below the critical U , the system is metallic even at $n=1$, and hence can also be superconducting at half-filling. This is seen in our calculations which give a finite order parameter at $n=1$ (see Fig. 5). We like to stress that close to half-filling the solution with lowest energy is always a mixed AF+SC one.³⁴ We checked this by comparing this solution to the pure AF and SC ones.

It is obvious that our determination of U_c is not as precise as it can be done by other methods, e.g., the path-integral renormalisation group.³⁷ Moreover, with the cluster sizes available in the present form of the VCA, it is not possible to detect whether or not we have a MQCP (Refs. 26 and 27) with a diverging charge susceptibility κ at the metal-insulator boundary. Nevertheless, our calculation allows to make a qualitative connection of the MIT and PS. It indicates that the collapse of the upper and lower dopings n_1 and n_2 (i.e., the disappearance of PS) and the closing of the Mott gap occur at almost the same critical interaction strength. It appears that it is important to have a Mott insulator at half-filling in order to get phase separation away from half-filling. Due to the limited cluster sizes available and the according

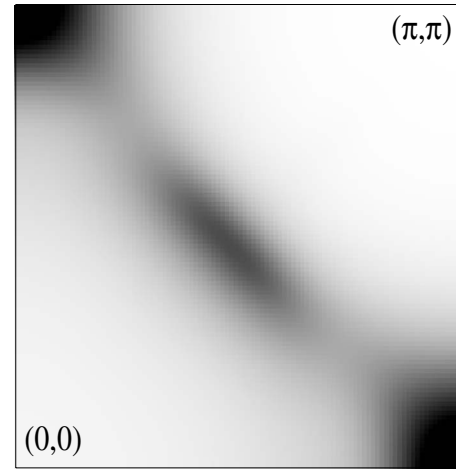


FIG. 7. Representation of the Fermi surface for an interaction $U=3.5 < U_c$ and $n=1$. Calculation using the $\sqrt{8} \times \sqrt{8}$ cluster. Dark regions denote large spectral weight integrated over a small frequency window of $\Delta\omega=\pm 0.05$ around $\omega=0$.

limited accuracy in the determination of critical points, however, this statement is somewhat speculative. Note that a relation between phase separation and the doping of a Mott insulator has been discussed in Ref. 32. There, it has been argued that a Mott insulator with broken symmetry, which is the $SU(2)$ symmetry in our case, enhances the possibility of PS.

In order to analyze the relation with single-particle excitations, we plot in Fig. 7 the Fermi surface for weak coupling, $U=3.5$, calculated with the $\sqrt{8} \times \sqrt{8}$ cluster. The closing of the Mott gap is clearly manifested by the occurrence of both hole and electron pockets near $(\pi/2, \pi/2)$ and $(\pi, 0)$, respectively, in direct contrast to the Fermi surface for larger coupling and $U=8$ where one has *either* hole *or* electron pockets at low doping.⁹ The simultaneous occurrence of hole and electron pockets has also been reported recently in weak-coupling calculations close to half-filling.³⁸

Another way to see the closing of the Mott gap is to look at the spectral function directly, which we plot in Fig. 8 for $U=8$ and $U=4$, respectively. Calculations have been done using the same $\sqrt{8} \times \sqrt{8}$ cluster as for Fig. 7, but at finite hole-doping just at the critical doping n_2 in the pure SC phase. From this figure, it is obvious that for $U=8$ one has a quasiparticle band at the Fermi level, well separated from the upper Hubbard band. For $U=4$, however, the upper and lower Hubbard bands merge, and closely resemble the band structure of the free system, except for the superconducting gap around $(\pi, 0)$.

Related ideas of a change of the type of the phase transition as a function of the interaction strength have been reported quite recently based on cellular DMFT calculations by Capone *et al.*¹¹ for the two-dimensional Hubbard model with $t_{\text{NNN}}=0$. Capone *et al.* inferred a critical interaction of approximately $U_c \approx 8$ below which the doping-dependent transition to a paramagnet is continuous and above which there is a first-order transition accompanied by phase separation. The U_c reported for $t_{\text{NNN}}=0$ and using cellular DMFT with 2×2 clusters is somewhat larger as in our study. A qualita-

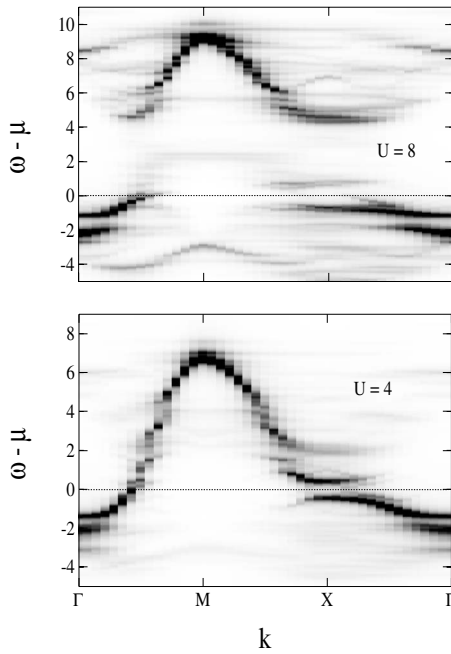


FIG. 8. Spectral function for $U=8$ (top) and $U=4$ (bottom). Calculation using a $\sqrt{8} \times \sqrt{8}$ cluster. The horizontal dashed line marks the chemical potential.

tive difference, however, is that we always find a mixed AF+SC state at low doping whereas the authors of Ref. 11 find a pure AF phase for strong interaction close to half-filling. One should note, however, that finding the stable solution with lowest energy can be a difficult task within quantum-cluster approaches. In Ref. 11 the calculation starts from pure AF and SC solutions and a mixed AF+SC solution is searched for by applying small perturbations to the pure ones. This procedure does not necessarily lead from one local solution to another, especially if the two are well separated in parameter space.

Finally, we would like to comment on the relation of our results to the t - J model. Translating our results of Fig. 3 to $J \propto t^2/U$, we argue that PS for small J (large U) should be weak, or eventually absent in the thermodynamic and $U \rightarrow \infty$ limit, since $\Delta\mu$ decreases significantly with increasing

U . However, from our results it is not possible to deduce a definite critical J_c below which PS should be absent. Nevertheless, the spectral function and in particular the low-lying quasiparticle band in our calculations is in well agreement with the low-lying bands in the t - J model.³⁹

IV. CONCLUSIONS

To summarize, we have studied the occurrence of phase separation in the two-dimensional Hubbard model at zero temperature depending on the strength of the Hubbard interaction U . We have employed the variational-cluster approach using clusters of different shapes and sizes up to 10 sites. Our results show that the nature of the doping-dependent transition from the antiferromagnetic and superconducting state to a nonmagnetic and purely superconducting state changes from discontinuous to continuous when going from the strong- and intermediate- to the weak-interaction regime. Below a critical value for the interaction strength no phase separation can be found. Above the critical value, there is a clear discontinuity in the density as a function of the chemical potential with a small finite-size error only. This is a strong indication that PS, or at least a phase with mesoscopic inhomogeneities, should persist in the thermodynamic limit, as long as the interaction is sufficiently strong.

We also studied the interaction-driven Mott transition at half-filling. For weak interactions (and $t_{\text{NNN}} = -0.3t_{\text{NN}}$) the system is in a mixed AF+dSC state with a finite charge susceptibility. The transition to the AF Mott insulator with vanishing charge susceptibility takes place at $U \approx 3.5$ –4. As the Mott transition at half-filling takes place at the same interaction strength where phase separation appears in the doped case, one might speculate that these two phenomena are closely related.

ACKNOWLEDGMENTS

The authors thank M. Imada for his valuable comments on the manuscript. This work has been supported by the Deutsche Forschungsgemeinschaft within the Forschergruppe FOR 538, by the Austrian science fund (FWF project P18551-N16), and in part by the National Science Foundation under Grant No. PHY 05-51164.

*aichhorn@physik.uni-wuerzburg.de

¹T. Maier, M. Jarrell, T. Pruschke, and M. H. Hettler, *Rev. Mod. Phys.* **77**, 1027 (2005).

²M. H. Hettler, A. N. Tahvildar-Zadeh, M. Jarrell, T. Pruschke, and H. R. Krishnamurthy, *Phys. Rev. B* **58**, R7475 (1998).

³G. Kotliar, S. Y. Savrasov, G. Pálsson, and G. Biroli, *Phys. Rev. Lett.* **87**, 186401 (2001).

⁴A. I. Lichtenstein and M. I. Katsnelson, *Phys. Rev. B* **62**, R9283 (2000).

⁵M. Potthoff, M. Aichhorn, and C. Dahnken, *Phys. Rev. Lett.* **91**, 206402 (2003).

⁶T. A. Maier, M. Jarrell, T. C. Schulthess, P. R. C. Kent, and J. B.

White, *Phys. Rev. Lett.* **95**, 237001 (2005).

⁷D. Sénéchal, P. L. Lavertu, M. A. Marois, and A.-M. S. Tremblay, *Phys. Rev. Lett.* **94**, 156404 (2005).

⁸M. Aichhorn and E. Arrigoni, *Europhys. Lett.* **72**, 117 (2005).

⁹M. Aichhorn, E. Arrigoni, M. Potthoff, and W. Hanke, *Phys. Rev. B* **74**, 024508 (2006).

¹⁰M. Aichhorn, E. Arrigoni, M. Potthoff, and W. Hanke, *Phys. Rev. B* **74**, 235117 (2006).

¹¹M. Capone and G. Kotliar, *Phys. Rev. B* **74**, 054513 (2006).

¹²J. M. Tranquada, B. J. Sternlieb, J. D. Axe, Y. Nakamura, and S. Uchida, *Nature (London)* **375**, 561 (1995).

¹³J. M. Tranquada, J. D. Axe, N. Ichikawa, Y. Nakamura, S.

- Uchida, and B. Nachumi, Phys. Rev. B **54**, 7489 (1996).
- ¹⁴M. Vershinin, S. Misra, S. Ono, Y. Abe, Y. Ando, and A. Yazdani, Science **303**, 1995 (2004).
- ¹⁵J. E. Hoffman, E. W. Hudson, K. M. Lang, V. Madhavan, H. Eisaki, S. Uchida, and J. C. Davis, Science **295**, 466 (2002).
- ¹⁶T. Hanaguri, C. Lupien, Y. Kohsaka, D. H. Lee, M. Azuma, M. Takano, H. Takagi, and J. C. Davis, Nature (London) **430**, 1001 (2004).
- ¹⁷K. McElroy, D. H. Lee, J. E. Hoffman, K. M. Lang, J. Lee, E. W. Hudson, H. Eisaki, S. Uchida, and J. C. Davis, Phys. Rev. Lett. **94**, 197005 (2005).
- ¹⁸U. Löw, V. J. Emery, K. Fabricius, and S. A. Kivelson, Phys. Rev. Lett. **72**, 1918 (1994).
- ¹⁹E. Arrigoni, A. P. Harju, W. Hanke, B. Brendel, and S. A. Kivelson, Phys. Rev. B **65**, 134503 (2002).
- ²⁰S. A. Kivelson, I. P. Bindloss, E. Fradkin, V. Oganessian, J. M. Tranquada, A. Kapitulnik, and C. Howald, Rev. Mod. Phys. **75**, 1201 (2003).
- ²¹A. Moreo, D. Scalapino, and E. Dagotto, Phys. Rev. B **43**, 11442 (1991).
- ²²F. Becca, M. Capone, and S. Sorella, Phys. Rev. B **62**, 12700 (2000).
- ²³R. Zitzler, T. Pruschke, and R. Bulla, Eur. Phys. J. B **27**, 473 (2002).
- ²⁴P. Werner and A. J. Millis, Phys. Rev. B **75**, 085108 (2007).
- ²⁵M. Eckstein, M. Kollar, M. Potthoff, and D. Vollhardt, Phys. Rev. B **75**, 125103 (2007).
- ²⁶M. Imada, Phys. Rev. B **72**, 075113 (2005).
- ²⁷T. Misawa and M. Imada, Phys. Rev. B **75**, 115121 (2007).
- ²⁸A. Macridin, M. Jarrell, and T. Maier, Phys. Rev. B **74**, 085104 (2006).
- ²⁹R. Preuss, W. Hanke, and W. von der Linden, Phys. Rev. Lett. **75**, 1344 (1995).
- ³⁰C. Gröber, M. G. Zacher, and R. Eder, arXiv:cond-mat/9810246 (unpublished).
- ³¹D. Sénéchal and A.-M. S. Tremblay, Phys. Rev. Lett. **92**, 126401 (2004).
- ³²D. H. Lee and S. A. Kivelson, Phys. Rev. B **67**, 024506 (2003).
- ³³M. Potthoff, Eur. Phys. J. B **32**, 429 (2003).
- ³⁴A mixed AF+SC phase has been first obtained by cluster methods in Ref. 4, and has been observed experimentally in Ref. 40 and recently in Ref. 41.
- ³⁵M. Aichhorn, H. G. Evertz, W. von der Linden, and M. Potthoff, Phys. Rev. B **70**, 235107 (2004).
- ³⁶S. Onoda and M. Imada, Phys. Rev. B **67**, 161102(R) (2003).
- ³⁷T. Mizusaki and M. Imada, Phys. Rev. B **74**, 014421 (2006).
- ³⁸J. Reiss, D. Rohe, and W. Metzner, Phys. Rev. B **75**, 075110 (2007).
- ³⁹For a recent work on the t - J -model, see: M. M. Zempljic, P. Prelovsek, and T. Tohyama, arXiv:0706.1156 (unpublished).
- ⁴⁰P. Dai, H. J. Kang, H. A. Mook, M. Matsuura, J. W. Lynn, Y. Kurita, S. Komiya, and Y. Ando, Phys. Rev. B **71**, 100502(R) (2005).
- ⁴¹W. Yu, J. S. Higgins, P. Bach, and R. L. Greene, Phys. Rev. B **76**, 020503(R) (2007).